ACS OMEGA

http://pubs.acs.org/journal/acsodf

Article

Enhanced Dopamine Sensitivity Using Steered Fast-Scan Cyclic Voltammetry

Yumin Kang,[#] Abhinav Goyal,[#] Sangmun Hwang, Cheonho Park, Hyun U. Cho, Hojin Shin, Jinsick Park, Kevin E. Bennet, Kendall H. Lee, Yoonbae Oh,[*] and Dong Pyo Jang[*]

Cite This: https://doi.org/10.1021/acsomega.1c04475

Read Online

ACCESS | Metrics & More | Article Recommendations

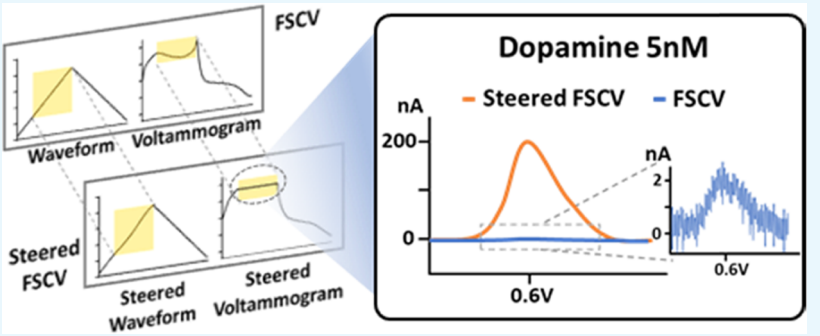

ABSTRACT: Fast-scan cyclic voltammetry (FSCV) is a technique for measuring phasic release of neurotransmitters with millisecond temporal resolution. The current data are captured by carbon fiber microelectrodes, and non-Faradaic current is subtracted from the background current to extract the Faradaic redox current through a background subtraction algorithm. FSCV is able to measure neurotransmitter concentrations *in vivo* down to the nanomolar scale, making it a very robust and useful technique for probing neurotransmitter release dynamics and communication across neural networks. In this study, we describe a technique that can further lower the limit of detection of FSCV. By taking advantage of a "waveform steering" technique and by amplifying only the oxidation peak of dopamine to reduce noise fluctuations, we demonstrate the ability to measure dopamine concentrations down to 0.17 nM. Waveform steering is a technique to dynamically alter the input waveform to ensure that the background current remains stable over time. Specifically, the region of the input waveform in the vicinity of the dopamine oxidation potential (~0.6 V) is kept flat. Thus, amplification of the input waveform will amplify only the Faradaic current, lowering the existing limit of detection for dopamine from 5.48 to 0.17 nM, a 32-fold reduction, and for serotonin, it lowers the limit of detection from 57.3 to 1.46 nM, a 39-fold reduction compared to conventional FSCV. Finally, the applicability of steered FSCV to *in vivo* dopamine detection was also demonstrated in this study. In conclusion, steered FSCV might be used as a neurochemical monitoring tool for enhancing detection sensitivity.

INTRODUCTION

Dopamine (DA) is an essential neurotransmitter in the brain, responsible for modulating a wide array of functions, including motivation, pleasure, and movement.[1,2] Dysfunction in dopaminergic dynamics is known to play a critical underlying role in several neuropathological disorders such as Parkinson's disease, addiction, obsessive-compulsive disorder, and Tourette's syndrome.[3,4] Therefore, furthering our understanding of the mechanisms of DA release and transmission in the central nervous system is of great importance to inform future development of therapies for these disorders. To measure DA in the brain in real-time, microdialysis and electrochemical methods are typically employed.[5,6] The former has been primarily utilized for sampling DA with high selectivity and sensitivity. While it boasts subnanomolar sensitivity and high selectivity using high-performance liquid chromatography, it suffers from low spatiotemporal resolution. Measurements can be taken once every minute,[7] at best, and the high diameter of the microdialysis cannula leads to a low spatial resolution as well as tissue damage. This tissue damage has been shown to confound *in vivo* measurements.[8] All of these drawbacks taken together limit future application for microdialysis for probing *in vivo* neurotransmitter dynamics.

Received: August 17, 2021
Accepted: November 16, 2021

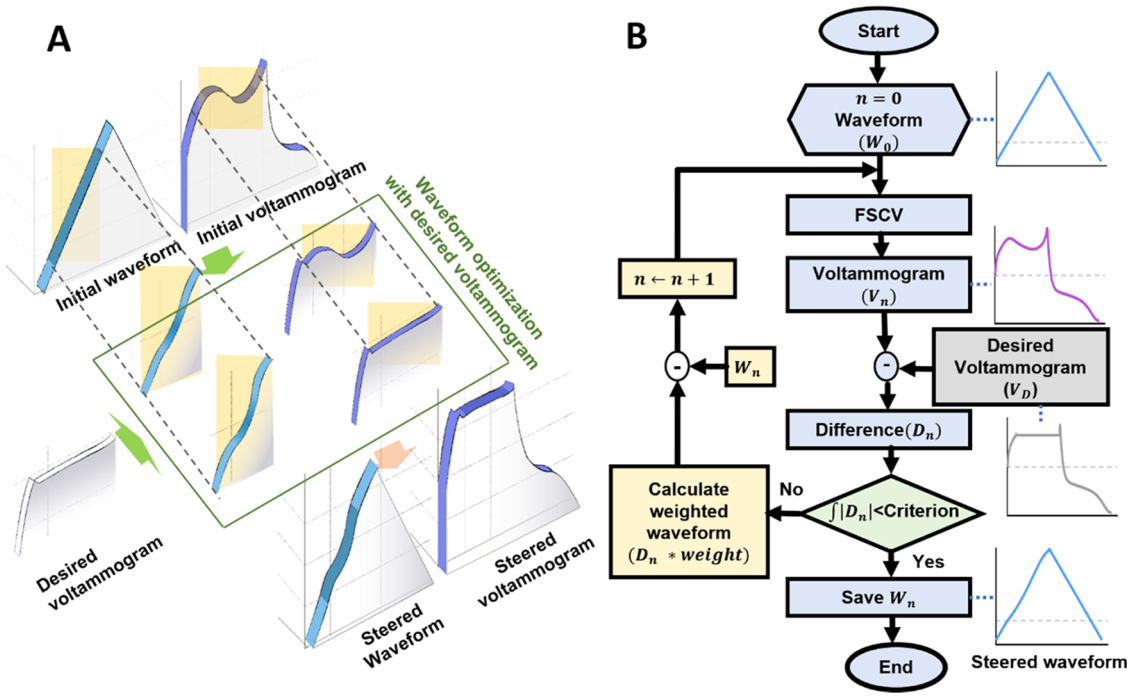

Figure 1. Description of the waveform steering technique. (A) The initial voltammogram is the output of the initial input waveform. When waveform optimization is performed using the desired voltammogram, a steered input waveform is generated to generate a steered voltammogram of the same shape as the desired voltammogram. (B) Feedback algorithm for deriving the steered input waveform. By comparing the desired voltammogram with the output voltammogram from the input waveform, the input waveform is iteratively updated to generate a steered waveform to output the desired voltammogram.

In contrast, electrochemical methods combined with carbon fiber microelectrodes boast high spatiotemporal resolution. For example, fast-scan cyclic voltammetry (FSCV) utilizes a triangular input voltammetric waveform that sweeps from −0.4 to 1.3 V at 400 V/s, with a scan repetition time of 10 Hz.[9,10] Carbon fiber microelectrodes have diameters of less than 10 μm, minimizing tissue damage and inflammation,[11] both of which can confound *in vivo* measurements. For these reasons, FSCV has been utilized for decades as the preferred method to measure synaptic release of DA and other neurotransmitters *in vivo*, both in animals and in humans. In addition, recent technical advancements in FSCV have been made to meet biological needs to measure low concentrations of neurotransmitters with high specificity by waveform optimization, material development, and signal processing.[9,12] Although the sensitivity of FSCV has been improved since its inception, there is still demand for improvement to enable further investigation into biological phenomena. The current limit of detection of FSCV algorithms, assuming an optimized research set up with limited noise, has been reported to be around 15 nM at carbon fiber microelectrodes.[10,13] Unfortunately, this is still insufficient for certain applications, such as measuring spontaneous (noninduced) neurotransmitter release.[14−16]

Previous attempts to increase FSCV sensitivity have employed a variety of methods, including increasing the scan rate[17] and utilizing square-wave voltammetry with relatively large amplitude and sampling rate (1 mega sample/s).[18] The limit of detection has been lowered to 0.17 nM using multiple cyclic-square-wave voltammetry, but this technique was designed to only measure tonic resting levels of neurotransmitters, and not phasic release.[19] In addition, square-wave voltammetry employs waveforms with a relatively low temporal resolution (1 scan every few seconds), so the technique lacks the temporal resolution necessary to record spontaneous activity, which occurs several times per second.[14] Another noteworthy attempt to increase sensitivity to DA was by changing the shape of the input waveform, and amplifying it, to change the shape of the resultant voltammogram.[20] This was able to reduce the limit of detection to DA down to 127 pM; however, the technique employed made use of a specially prepared potentiostat for use in *in vitro* solutions, and it has not been tested in the *in vivo* environment. Further, the algorithm for generating a particular voltammogram was not discussed and the waveform optimization procedure takes up to 10 min.

In this study, we employ a waveform steering technique to control the input waveform to modify the resultant voltammogram to achieve a flat background current at voltages near the oxidation potential of DA (~0.6 V). A preamplifier specifically designed to amplify only the oxidation current from the redox currents obtained from the steered input waveform is also discussed. This technique lowers the limit of detection of DA to 0.17 nM (170 pM) and is employable both *in vitro* and *in vivo*, making it a very useful modification to FSCV for applications requiring a very low limit of detection.

RESULTS AND DISCUSSION

Waveform Steering Technique. The waveform steering technique is designed to induce a desired shape of a voltammogram by modifying the input waveform during conventional FSCV (Figure 1). Figure 1A shows that the voltammogram changes as the waveform and properties required for the waveform steering technique change. When the initial waveform is input, the initial voltammogram is output and the waveform is changed through comparison with

https://doi.org/10.1021/acsomega.1c04475
ACS Omega XXXX, XXX, XXX−XXX

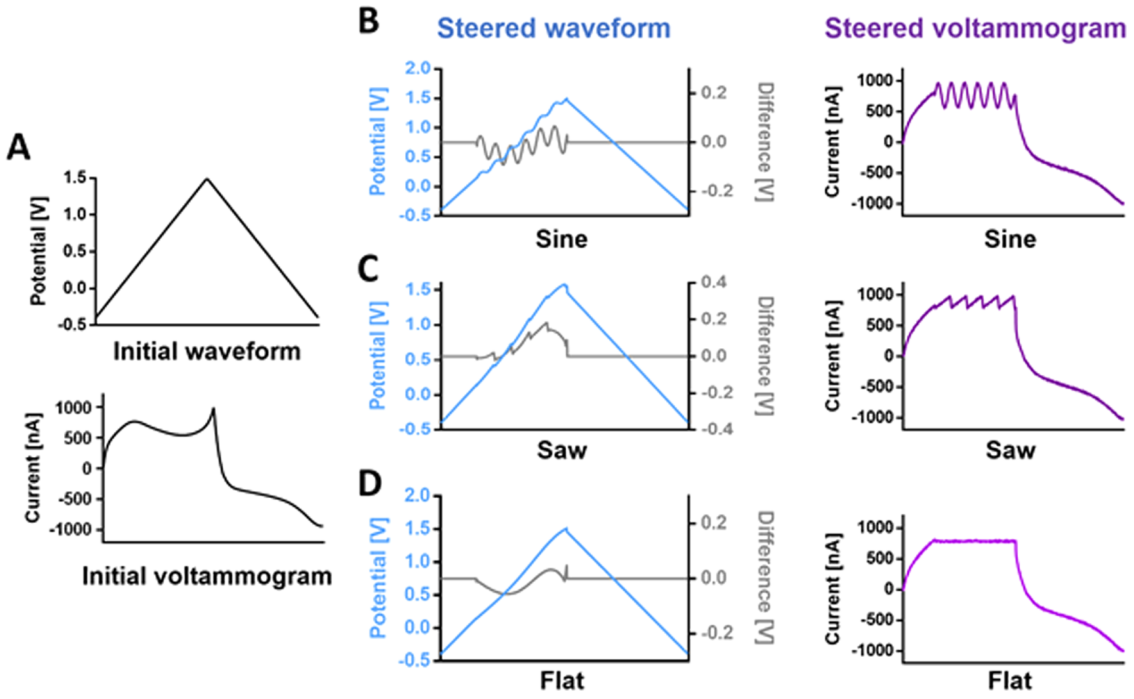

Figure 2. Output voltammograms from various input waveforms. (A) Triangle waveform used to perform conventional FSCV. (B, C) Difference (gray) between the steered waveform (blue) used to acquire a steered voltammogram (purple) including sine wave or saw tooth wave and the initial waveform used in conventional FSCV. (D) Difference (gray) between the steered waveform (blue) to derive a voltammogram with a flat oxidation region.

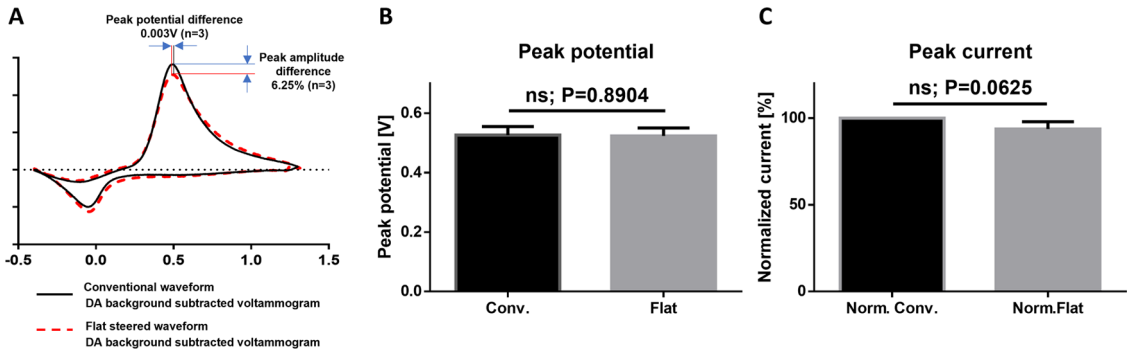

Figure 3. Change in DA response to different input waveforms (original triangle waveform and flat steered waveform). (A) Background-subtracted voltammograms obtained using conventional FSCV (black) and a flat steered waveform (red). (B) The location of the oxidation peak of DA shows a difference of about 3 mV. (C) The amplitude of the currents shows no significant difference.

the desired voltammogram. Finally, when the optimized steered waveform is input, a steered voltammogram in the same form as the desired voltammogram can be obtained. Figure 1B shows the algorithm for generating a steered waveform. The initial input waveform (W_0) can be of any form, but here, the standard FSCV waveform is depicted. The voltammogram obtained with this waveform is then subtracted from the desired voltammogram V_D to obtain a difference D_N, where N is the iteration number. The area of this difference over the desired section (the vicinity of the DA oxidation potential) is then compared to a preestablished criterion. If the difference exceeds the minimum criterion, it is multiplied by a weighting factor that is determined in advance. Weighting factors can range from 0.001 to 0.005. A smaller weighting factor will lead to a highly optimized input waveform, at the cost of an increased number of iterations, leading to longer optimization time. This weighting serves to adjust the waveform to be applied on the next iteration. The time to generate the optimized steered waveform differs depending on the voltammogram type and weight setting, but since FSCV applies the waveform every 100 ms, the waveform is usually optimized within 10 s.

Using the waveform steering technique, various types of voltammograms can be derived. Figure 2A shows the voltammogram that can be obtained using the conventional triangular waveform, and the middle column shows the steered waveform (blue solid line) to obtain voltammograms of sine wave (Figure 2B), saw tooth wave (Figure 2C), and flat form (Figure 2D). The right column shows the voltammogram that results from the input waveform in the middle column. From this, it is seen that any desired voltammogram shape can be generated using the waveform steering technique. One interesting point is that the difference between the initial waveform and the flat steered waveform was quite small (range < 0.05 V; Figure 2D, gray, solid line).

https://doi.org/10.1021/acsomega.1c04475
ACS Omega XXXX, XXX, XXX−XXX

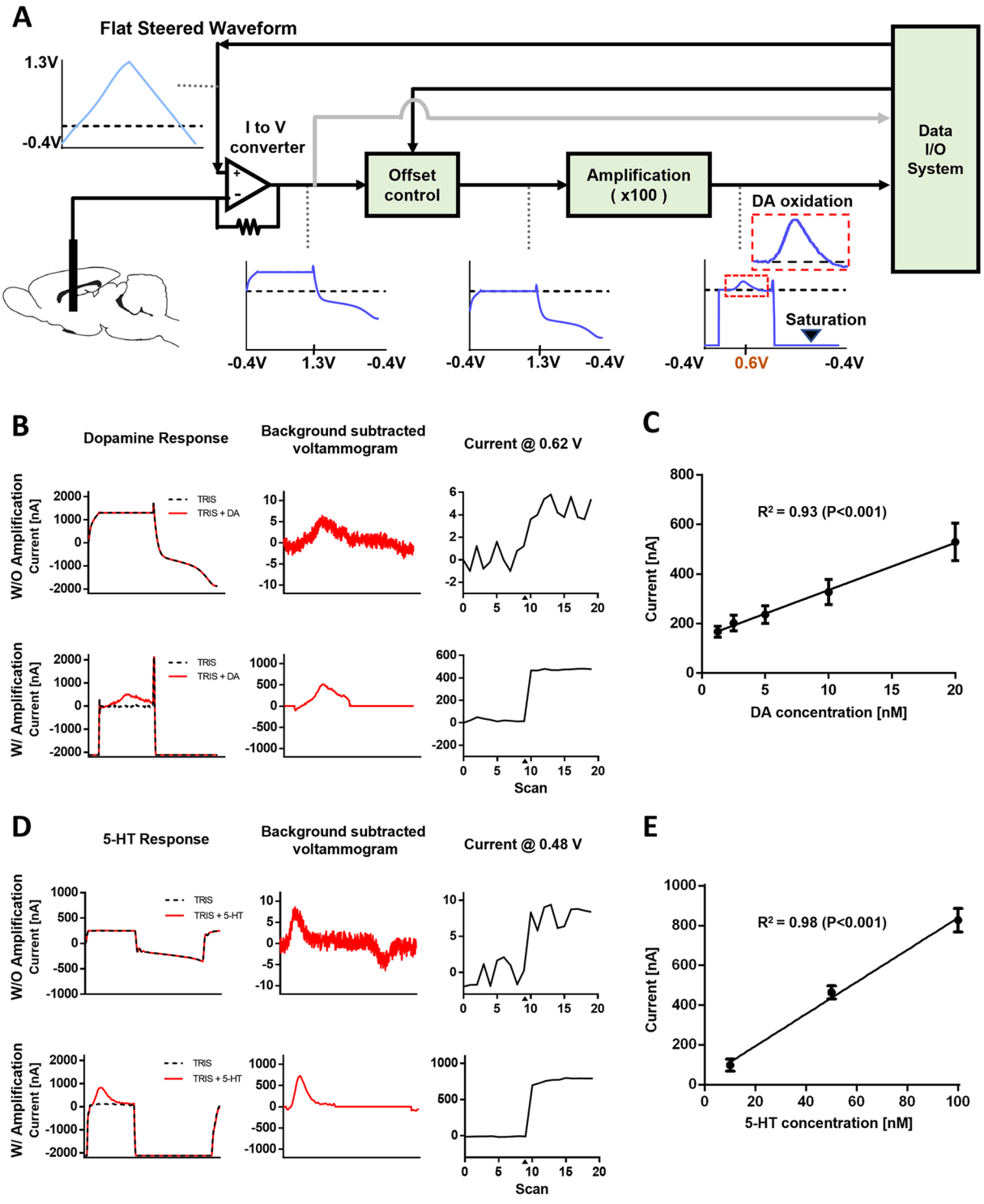

Figure 4. Signal processing and dopamine and 5-HT response using the preamplifier. (A) Block diagram demonstrating the steps to alter the voltammogram. A flat voltammogram can be obtained by applying the steered waveform. The flat potential is adjusted to 0 V using an offset controller and amplified 100 times using an extra-amplifier. The dopamine oxidation peak is then measured from the flat part. (B) The upper row is the result of obtaining a flat dopamine voltammogram derived using a flat steered waveform and analyzing it using the background subtraction technique, and the lower row is the result of analyzing the Faradaic current after amplification. The left column shows the voltammogram, the black dotted line shows the non-Faradaic current, and the red solid line shows the Faradaic current at 20 nM of DA. The middle column shows the Faradaic current obtained from background subtraction. The right column shows the change in Faradaic current at 0.62 V over time. (C) Current resulting from 1.25, 2.5, 5, 10, and 20 nM dopamine after amplification. (D) The upper row is the result of obtaining a flat 5-HT voltammogram derived using a flat steered waveform and analyzing it using the background subtraction technique, and the lower row is the result of analyzing the Faradaic current after amplification. The left column shows the voltammogram and waveform, the black solid line shows the Faradaic current at 100 nM of 5-HT, and the gray solid line shows the N-shape waveform. The right column shows the change in Faradaic current at 0.48 V over time. (E) Current resulting from 10, 50, and 100 nM 5-HT after amplification.

https://doi.org/10.1021/acsomega.1c04475
ACS Omega XXXX, XXX, XXX−XXX

In conventional FSCV, the magnitude of the non-Faradaic current is significantly larger than that of the Faradaic current. Thus, a large amplification must be used to measure the concentration of a small amount of neurotransmitter. In this case, since the magnitude of the non-Faradaic current also increases, it may be impossible to measure beyond the measurement range of the analog-to-digital converter (ADC). Therefore, by flattening the non-Faradaic current (Figure 2D), the change in the size of the current due to amplification can be effectively ignored. It is important to derive a flat steered voltammogram by applying a waveform steering technique because the DC-type current can be selectively removed using a preamplifier.

To derive the desired voltammogram using the waveform steering technique, a waveform with a variable scan rate was used, as opposed to the constant scan rate used in conventional FSCV. Figure 3A shows the output voltammograms of the conventional triangular waveform (increasing from −0.4 to 1.3 V at a rate of 400 V/s and returning to −0.4 V at a rate of 400 V/s; black line) and the steered waveform to obtain a flat voltammogram (red dotted line). The potential where the peak Faradaic current occurs and the magnitude of the peak Faradaic current were only slightly changed between the two waveforms (Figure 3B,C). The average difference of this peak potential between the two waveforms was about 3 mV and not significantly different (Figure 3B, unpaired *t*-test, $n = 3$, $p = 0.89$). Dopamine sensitivity to these waveforms was not also significantly different (Figure 3C, unpaired *t*-test, $n = 3$, $p = 0.062$). The change in the peak potential position depends on the shape of the waveform used to create the steered voltammogram, specifically relating to the rate of change of the waveform scan rate in the vicinity of the oxidation peak of DA. A high rate of change of the scan rate enables the steered waveform to more quickly reach the peak potential so that the oxidation peak will occur at a lower absolute potential, and vice versa; however, the differences are nonsignificant, indicating that this technique can be safely used to measure DA concentrations.

Offset Control and Amplification of Steered Fast-Scan Cyclic Voltammetry. To amplify only the Faradaic current generated from the oxidation of dopamine, a special type of preamplifier is required; its composition and function are shown in Figure 4A. The preamplifier consists of a current-to-voltage converter (IVC), an offset controller, and an extra-amplifier. All analog devices are manufactured using a low-noise operational amplifier (OPA2604, Texas Instruments). The IVC applies the steered voltammogram output from the data I/O system to the carbon fiber microelectrode and converts the resulting nanocurrent back to voltage. When amplifying in this state, the potential should be lowered to 0 V because there is a high possibility that a flat part with a positive potential would exceed the measurement range of the Data I/O system. The offset controller handles this problem. Adjusting the potential of the flat part of the steered voltammogram to 0 V has the same effect as removing the background current of the flat steered voltammogram using an analog circuit. The extra-amplifier then amplifies the adjusted flat part of the voltammogram. Because the location of Faradaic current generation due to the oxidation of dopamine was adjusted to 0 V through the offset controller, 0 V can be maintained despite passing through the extra-amplifier. If dopamine is present, the Faradaic current generated by the oxidation of dopamine appears as a hump above the flat baseline (red box, Figure 4A). The amplification of the extra-amplifier can be changed depending on the concentration of dopamine to be measured or the measurement range of the ADC of the Data I/O system. In this study, a 100-fold amplification was used.

Figure 4B shows the steered FSCV response to 20 nM of DA before and after amplification. The upper row shows the dopamine response before amplification, and the lower row shows the dopamine response after passing through the offset controller and extra-amplifier. The left column shows the total voltammogram generated when a steered waveform is applied. The black dotted line is the current response in the absence of dopamine, and the red solid line is the current response in the presence of dopamine. The middle column shows only the Faradaic current generated by dopamine redox using background subtraction. The right column displays the dopamine response at 0.62 V. The triangle mark below the *X*-axis indicates the injection time of dopamine into the flow cell. In conventional FSCV, the limit of detection (LoD) is calculated as the ratio of 3*std of the temporal change of non-Faradaic current to the magnitude of the dopamine response. Therefore, if the change in the non-Faradaic current is small, the LoD will be lowered. In buffer, the magnitude of the change in the non-Faradaic current generated in conventional FSCV is 0.04 ± 0.95 nM (mean ± std.); using steered FSCV, it is 4.38 ± 3.99 nM. Using steered FSCV, the preamplifier was used to amplify the voltammogram by 100×, but the standard deviation only increased about 4.2×, mainly stemming from the amplified background noise. Therefore, LoD can be decreased by 32-fold compared to conventional FSCV (5.48 nM down to 0.17 nM). Figure 4C shows the dopamine current response vs concentration in the flow cell. DA concentrations were 1.25, 2.5, 5, 10, and 20 nM, with $n = 3$ per concentration. The calibration curve showed a linear pattern ($R^2 = 0.93$, $p < 0.001$).

Figure 4D shows the steered FSCV response to 100 nM of 5-HT before and after amplification. The upper row shows the 5-HT response before amplification, and the lower row shows the 5-HT response after passing through the offset controller and extra-amplifier. The left column shows only the Faradaic current generated by 5-HT redox using background subtraction. The right column displays the 5-HT response at 0.48 V. The triangle mark below the *X*-axis indicates the injection time of 5-HT into the flow cell. LoD can be decreased by 39-fold compared to conventional FSCV (57.3 nM down to 1.46 nM) These results imply that Steered FSCV can improve the detection sensitivity for many neurotransmitters by modifying various waveforms. Figure 4E shows the 5-HT current response vs concentration in the flow cell. 5-HT concentrations were 10, 50, and 100 nM, with $n = 3$ per concentration. The calibration curve showed a linear pattern ($R^2 = 0.98$, $p < 0.001$).

As the DA concentration decreases, the magnitude of the Faradaic current decreases. In general, if the magnitude of the temporal noise (fluctuations in successive DA current measurements) is larger than the change caused by the Faradaic current, dopamine cannot be detected. In this study, when a signal is amplified using a flat voltammogram, a low concentration of dopamine can be detected because the amount of amplification of the magnitude of the Faradaic current surpasses the temporal noise.

***In Vivo* Application of Steered FSCV.** This technique was then verified *in vivo* (Figure 5A). To verify the

https://doi.org/10.1021/acsomega.1c04475
ACS Omega XXXX, XXX, XXX−XXX

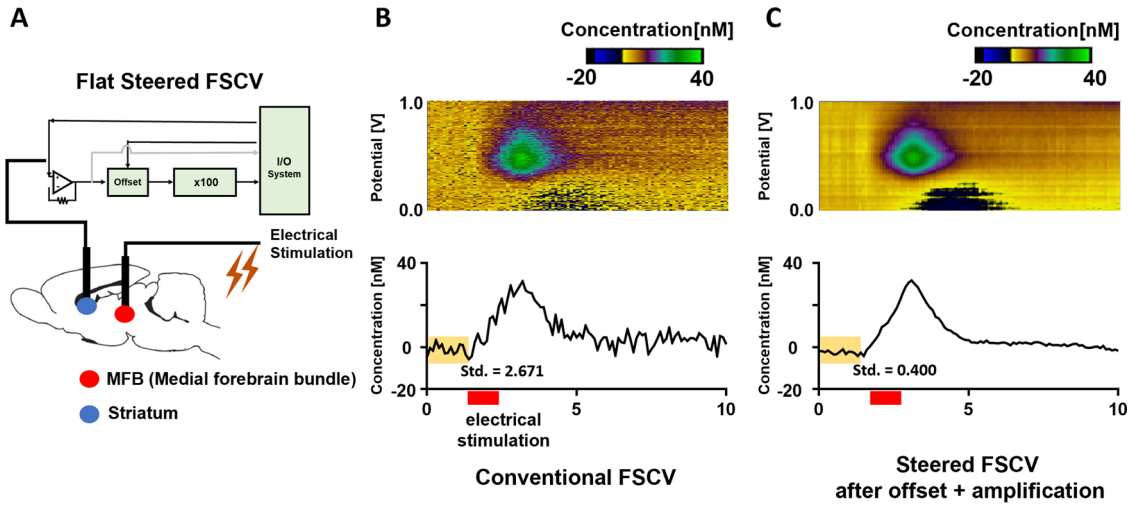

Figure 5. In vivo experiment results using Steered FSCV. (A) A carbon fiber microelectrode is located in the dorsal striatum, and electrical stimulation is applied to the medial forebrain bundle (MFB). DA response measured using (B) conventional FSCV and (C) Steered FSCV with amplification. A total of 10 s before and after stimulation was measured, with the position of the stimulation indicated by a red bar.

effectiveness of detection of dopamine induced by electrical stimulation, the stimulation parameters were set to 2 ms pulse width, 60 Hz, 100 μA, and stimulation was delivered for 1 s. In Figure 5B,C, the upper row shows a color plot of dopamine response pre- and post-stimulation and the lower row shows the temporal change in dopamine oxidation current at 0.6 V. The dopamine response to MFB stimulation was about 32 nM as shown in Figure 5B. Using standard FSCV, the value of the current cannot be precisely determined due to the surrounding noise. *In vivo* especially, it is difficult to measure very low dopamine concentrations due to the large influence of noise. However, the Steered FSCV technique is able to mitigate the influence of noise by amplifying only the Faradaic current, making the dopamine current response much easier to analyze. Both signals (Figure 5B,C) have the same concentration because they were measured simultaneously at the same spot, but with different standard deviations of the temporal change: Conventional FSCV Std 2.67 nM and Steered FSCV Std 0.40 nM. This makes it possible to estimate small dopamine concentrations a 6.7-fold more accurately *in vivo*.

CONCLUSIONS

In this study, we have developed a technology that can induce various types of voltammograms by adjusting the input waveform using the waveform steering technique. By generating an output voltammogram with a flat response in the dopamine oxidation region, and by constructing a preamplifier that was able to amplify the current only from this voltage range, we were able to lower the limit of detection of dopamine, both *in vitro* down to 0.17 nM, a 32-fold reduction, and *in vivo* down to 1.2 nM, a 6.7-fold reduction compared to conventional FSCV. The waveform steering technique can be applied to any waveform, such as the N-shape waveform for detecting 5-HT. It lowers the limit of detection of 5-HT *in vitro* down to 1.46 nM, a 39-fold decrease compared to the conventional N-shape FSCV.

METHODS

FSCV Input Waveform. Steered FSCV requires the use of conventional FSCV, which uses a waveform that increases from −0.4 to 1.3 V at a rate of 400 V/s and then returns to −0.4 V (Figure 1). The input waveform is about 8.5 ms long and is applied every 100 ms.

Data I/O System and Analysis. After application of the input waveform, the resulting electrochemical redox data were collected by the carbon fiber microelectrode and passed through a preamplifier to an NI-DAQ board (NI USB-6251, 16-bit, National Instrument). The output range of the digital-to-analog converter (DAC) for controlling the waveform output and the offset controller is ±10 V, and the input range of the analog-to-digital converter (ADC) for receiving the voltammogram is ±10 V, and each has a resolution of 16 bits. The NI-DAQ board passed the resultant digital data to the computer for analysis.

Custom acquisition software was written using LabVIEW 2016 and has functions to adjust the FSCV input waveform parameters, implement the waveform steering technique through NI USB-6251 control, and synchronize the flow injection apparatus. Using two analog input channels, the output values from the current-to-voltage converter (IVC) and the extra-amplifier module were simultaneously acquired in the form of 2 byte signed integer. The raw data are continuously saved to the hard drive. For postprocessing, the saved data were analyzed with custom software written in LabVIEW 2016, and has signal processing and data display functions such as background subtraction and filtering. All figures were prepared using GraphPad Prism 6 (GraphPad Software, San Diego, CA).

Flow Cell Apparatus. A flow injection system was used for in vitro experiments. The flow injection system was composed of a syringe pump (Harvard Apparatus, Hollisoton, MA), a six-port switching valve (Rheodyne, Rohnert Park, CA), and an electrochemical flow cell, all connected using Teflon tubing. The syringe pump was set at a flow rate of 2 ml/min, the carbon fiber microelectrode (CFM) was placed in the center of the flow cell, and the injection of buffer solution and analyte was controlled by controlling the six-port switching valve. The six-port switching valve was connected to the DO port of the NI-DAQ system and synchronized with the waveform output.

Solutions. Dopamine, 5-HT, and Trizma base were purchased from Sigma-Aldrich (St. Louis, MO). Tris buffer was made as discussed previously.[18] Briefly, sodium chloride,

https://doi.org/10.1021/acsomega.1c04475
ACS Omega XXXX, XXX, XXX−XXX

Trizma base, water, and hydrochloric acid are mixed to achieve a buffered solution with pH = 7.4. Dopamine (1 mM) and 5-HT stock solutions were made by dissolving each neurotransmitter in Tris buffer, and each stock was used to create dilutions.

Fabrication of Carbon Fiber Microelectrodes. CFMs were fabricated using an established standardized CFM design previously reported.[15] Briefly, a single carbon fiber (AS4, diameter = 7 μm; Hexel, Dublin, CA) was inserted into a silica tube (20 μM ID, 90 μM OD, 10 μM coat with polyimide; Polymicro Technologies, Phoenix, AZ). The connection between the carbon fiber and the silica tubing was sealed with epoxy resin. The other end of the silica tubing was then attached to a nitinol (Nitinol #1, an alloy of nickel and titanium; Fort Wayne Metals, IN) extension wire with a silver-based conductive paste. The silica and nitinol wire were insulated with polyimide tubing (0.0089″ID, 0.0134″OD, 0.00225″ WT; Vention Medical, Salem, NH) up to the carbon fiber. The exposed carbon fiber was then trimmed under a dissecting microscope to a length of 50 μm. Teflon-coated silver (Ag) wire (A-M systems, Inc., Sequim, WA) was prepared as an Ag/AgCl counter-reference electrode by chlorinating the exposed tip in saline with a 9 V dry cell battery. CFMs were pretested in a flow cell prior to coating deposition with a PEDOT:Nafion deposition solution, which minimized the effect of *in vivo* biofouling.

***In Vivo* Experiments.** Male Sprague−Dawley rats were used for *in vivo* experiments. Rats were anesthetized with urethane (Sigma-Aldrich, 2.24 g/kg, i.p.) and head-fixed to a stereotactic frame (David Kopf Instruments, Tujunga, CA). One burr hole was made above the dorsal striatum (AP +1.2, ML 2.0, DV −4.5), one was made above the medial forebrain bundle (MFB; AP −4.6, ML 1.4, DV −8.4), and one was made in the contralateral cortex for reference electrode placement. A carbon fiber microelectrode was lowered to about 1 mm above the dorsal striatum, and a stimulating electrode (twisted bipolar stimulating electrode—Plastics One, MS 303/2, Roanoke, VA, with the tips separated by 1 mm) was lowered to the MFB. Optimal positioning of the carbon fiber microelectrode was determined by measuring the evoked DA signal in response to MFB stimulation (2 ms pulse width, 60 Hz, 300 μA, 1 s stimulation) and lowering the depth by 0.1 mm after each stimulation. Once the optimal depth was determined, data collection began. Dopamine was evoked in the dorsal striatum through electrical stimulation of the MFB every 10 min. Waveform steering was performed before each stimulation.

AUTHOR INFORMATION

Corresponding Authors

Yoonbae Oh − *Department of Neurologic Surgery, Mayo Clinic, Rochester, Minnesota 55905, United States; Department of Biomedical Engineering, Mayo Clinic, Rochester, Minnesota 55905, United States;* orcid.org/0000-0003-1779-978X; Phone: 507-293-7992; Email: oh.yoonbae@mayo.edu

Dong Pyo Jang − *Department of Biomedical Engineering, Hanyang University, Seoul 04763, Republic of Korea;* orcid.org/0000-0002-2832-2576; Email: dongpjang@hanyang.ac.kr

Authors

Yumin Kang − *Department of Biomedical Engineering, Hanyang University, Seoul 04763, Republic of Korea;* orcid.org/0000-0002-2758-2202

Abhinav Goyal − *Department of Neurologic Surgery, Mayo Clinic, Rochester, Minnesota 55905, United States; Mayo Clinic Medical Scientist Training Program, Mayo Clinic, Rochester, Minnesota 55905, United States*

Sangmun Hwang − *Department of Biomedical Engineering, Hanyang University, Seoul 04763, Republic of Korea*

Cheonho Park − *Department of Biomedical Engineering, Hanyang University, Seoul 04763, Republic of Korea*

Hyun U. Cho − *Department of Biomedical Engineering, Hanyang University, Seoul 04763, Republic of Korea*

Hojin Shin − *Department of Neurologic Surgery, Mayo Clinic, Rochester, Minnesota 55905, United States;* orcid.org/0000-0001-6095-5122

Jinsick Park − *Department of Biomedical Engineering, Hanyang University, Seoul 04763, Republic of Korea*

Kevin E. Bennet − *Department of Neurologic Surgery, Mayo Clinic, Rochester, Minnesota 55905, United States; Division of Engineering, Mayo Clinic, Rochester, Minnesota 55905, United States*

Kendall H. Lee − *Department of Neurologic Surgery, Mayo Clinic, Rochester, Minnesota 55905, United States; Department of Biomedical Engineering, Mayo Clinic, Rochester, Minnesota 55905, United States*

Complete contact information is available at: https://pubs.acs.org/10.1021/acsomega.1c04475

Author Contributions

#Y.K. and A.G. contributed equally to this work. Y.O. and D.P.J. supervised all aspects of this work equally.

Notes

The authors declare no competing financial interest.

ACKNOWLEDGMENTS

This research was supported by the National Research Foundation of Korea (NRF) grant (NRF-2021R1A2B5B02002437), the National Institute of Health (NIH) R01NS112176 award, and Minnesota Partnership for Biotechnology and Medical Genomics (MNP #19.13).

REFERENCES

(1) Arbuthnott, G. W.; Wickens, J. Space, time and dopamine. *Trends Neurosci.* **2007**, *30*, 62−69.

(2) Ungerstedt U, P. C. Functional correlates of dopamine neurotransmission. *Bull. Schweiz. Akad. Med. Wiss.* **1974**, *30*, 44−55.

(3) Burbulla, L. F.; Song, P.; Mazzulli, J. R.; Zampese, E.; Wong, Y. C.; Jeon, S.; Santos, D. P.; Blanz, J.; Obermaier, C. D.; Strojny, C.; Savas, J. N.; Kiskinis, E.; Zhuang, X.; Krüger, R.; Surmeier, D. J.; Krainc, D. Dopamine oxidation mediates mitochondrial and lysosomal dysfunction in Parkinson's disease. *Science* **2017**, *357*, 1255−1261.

(4) Rusheen, A. E.; Gee, T. A.; Jang, D. P.; Blaha, C. D.; Bennet, K. E.; Lee, K. H.; Heien, M. L.; Oh, Y. Evaluation of electrochemical methods for tonic dopamine detection in vivo. *TrAC, Trends Anal. Chem.* **2020**, *132*, No. 116049.

(5) Benveniste, H. Brain Microdialysis. *J. Neurochem.* **1989**, *52*, No. 1667.

(6) Darren Michael, E. R. T.; Wightman, R. M. Peer Reviewed_-Color Images for FSCV Measurements in Biological Systems *Analytical Chemistry News & Features*, 1998.

https://doi.org/10.1021/acsomega.1c04475
ACS Omega XXXX, XXX, XXX−XXX

(7) Gu, H.; Varner, E. L.; Groskreutz, S. R.; Michael, A. C.; Weber, S. G. In Vivo Monitoring of Dopamine by Microdialysis with 1 min Temporal Resolution Using Online Capillary Liquid Chromatography with Electrochemical Detection. *Anal. Chem.* **2015**, *87*, 6088−6094.
(8) Blaha, C. D.; Coury, A.; Phillips, A. G. Does Monoamine oxidase inhibitaion by pargyline increase extracellular dopamine in the striatum? *Neuroscience* **1996**, *75*, 543−550.
(9) Puthongkham, P.; Venton, B. J. Recent advances in fast-scan cyclic voltammetry. *Analyst* **2020**, *145*, 1087−1102.
(10) Venton, B. J.; Cao, Q. Fundamentals of fast-scan cyclic voltammetry for dopamine detection. *Analyst* **2020**, *145*, 1158−1168.
(11) Peters, J. L.; Miner, L. H.; Michael, A. C.; Sesack, S. R. Ultrastructure at carbon fiber microelectrode implantation sites after acute voltammetric measurements in the striatum of anesthetized rats. *J. Neurosci. Methods* **2004**, *137*, 9−23.
(12) DeWaele, M.; Oh, Y.; Park, C.; Kang, Y. M.; Shin, H.; Blaha, C. D.; Bennet, K. E.; Kim, I. Y.; Lee, K. H.; Jang, D. P. A baseline drift detrending technique for fast scan cyclic voltammetry. *Analyst* **2017**, *142*, 4317−4321.
(13) Puthongkham, P.; Yang, C.; Venton, B. J. Carbon Nanohorn-Modified Carbon Fiber Microelectrodes for Dopamine Detection. *Electroanalysis* **2018**, *30*, 1073−1081.
(14) Kavalali, E. T. The mechanisms and functions of spontaneous neurotransmitter release. *Nat. Rev. Neurosci.* **2015**, *16*, 5−16.
(15) Bouron, A. Modulation of spontaneous quantal release of neurotransmitters in the hippocampus. *Prog. Neurobiol.* **2001**, *63*, 613−635.
(16) Kaeser, P. S.; Regehr, W. G. Molecular mechanisms for synchronous, asynchronous, and spontaneous neurotransmitter release. *Annu. Rev. Physiol.* **2014**, *76*, 333−363.
(17) Keithley, R. B.; Takmakov, P.; Bucher, E. S.; Belle, A. M.; Owesson-White, C. A.; Park, J.; Wightman, R. M. Higher sensitivity dopamine measurements with faster-scan cyclic voltammetry. *Anal. Chem.* **2011**, *83*, 3563−3571.
(18) Park, C.; Oh, Y.; Shin, H.; Kim, J.; Kang, Y.; Sim, J.; Cho, H. U.; Lee, H. K.; Jung, S. J.; Blaha, C. D.; Bennet, K. E.; Heien, M. L.; Lee, K. H.; Kim, I. Y.; Jang, D. P. Fast Cyclic Square-Wave Voltammetry To Enhance Neurotransmitter Selectivity and Sensitivity. *Anal. Chem.* **2018**, *90*, 13348−13355.
(19) Oh, Y.; Heien, M. L.; Park, C.; Kang, Y. M.; Kim, J.; Boschen, S. L.; Shin, H.; Cho, H. U.; Blaha, C. D.; Bennet, K. E.; Lee, H. K.; Jung, S. J.; Kim, I. Y.; Lee, K. H.; Jang, D. P. Tracking tonic dopamine levels in vivo using multiple cyclic square wave voltammetry. *Biosens. Bioelectron.* **2018**, *121*, 174−182.
(20) Yoo, J. S.; Park, S. M. Programmed Potential Sweep Voltammetry for Lower Detection Limits. *Anal. Chem.* **2005**, *77*, 3694−3699.

https://doi.org/10.1021/acsomega.1c04475
ACS Omega XXXX, XXX, XXX−XXX